

AD-A215 384

1

STRUCTURAL INSTABILITIES, IMPURITIES AND DEFECTS IN ELECTRONIC MATERIALS

Final Report for Contract Period

15 August 1987 - 30 September 1989

DTIC
ELECTED
DEC 07 1989
S D
D as

Contract No. N00014-83-K-0535

Principal Investigator: P.C. Taylor

Associate Principal Investigator: William D. Ohlsen

Department of Physics
University of Utah
Salt Lake City, UT 84112

DISTRIBUTION STATEMENT A

**CUMULATIVE LIST FOR PUBLICATIONS FOR
CONTRACT NO. N00014-83-K-0535**

- 83-K-0535-1: "Photoluminescence Study of Confined Electron Hole Plasma in $\text{Ga}_x\text{In}_{1-x}\text{As}$ Heterostructures," M. Gal, J.M. Viner, P.C. Taylor, C.P. Kuo, R.M. Cohen and G.B. Stringfellow, *J. Appl. Phys.* **58**, 948 (1985).
- 83-K-0535-2: "Magnetic Effects in Non-Crystalline Semiconductors," P.C. Taylor in Amorphous Semiconductors, M. Pollak, ed. (CRC Press, NY, 1987), p. 69.
- 83-K-0535-3: "Nuclear Quadrupole Resonance in the Chalcogenide and Pnictide Amorphous Semiconductors," P.C. Taylor in Physics and Chemistry of Disordered Systems, D. Adler, H. Fritzsche, and S.R. Ovshinsky, eds. (Plenum, NY, 1985), p. 517.
- 83-K-0535-4: "Optical Properties of Non-Crystalline Semiconductors," P.C. Taylor in Amorphous Semiconductors, M. Pollak, ed. (CRC Press, NY, 1987), p. 19.
- 83-K-0535-5: "Defects in Tetrahedrally Coordinated Amorphous Semiconductors," P.C. Taylor in Materials Issues in Applications of Amorphous Silicon Technology, Vol. 49, D. Adler, A. Madan, and M.J. Thompson, eds. (Materials Research Society, Pittsburgh, 1985), p. 61.
- 83-K-0535-6: "Doping Superlattices in Organometallic VPE InP," J.S. Yuan, M. Gal, P.C. Taylor and G.B. Stringfellow, *Appl. Phys. Lett.* **47**, 405 (1985).
- 83-K-0535-7: "Modulated-Reflectance Spectroscopy of InP Doping Superlattices," M. Gal, J.S. Yuan, J.M. Viner, P.C. Taylor and G.B. Stringfellow, *Phys. Rev. Lett.* **B33**, 4410 (1986).
- 83-K-0535-8: "Thermally-Modulated Photoluminescence in GaInAs-InP Quantum Wells," M. Gal, C.P. Kuo, B. Lee, R. Ranganathan, P.C. Taylor and G.B. Stringfellow, *Phys. Rev. B* **34**, 1356 (1986).
- 83-K-0535-9: "Defects and the Photodarkening Process in the Chalcogenide Glasses," P.C. Taylor and J.Z. Liu, in Defects in Glasses, F.L. Galeener, D.L. Griscom and M. Weber, eds., Symposia Proceedings, Vol. 61 (Materials Research Society, Pittsburgh, 1986), p. 223.
- 83-K-0535-10: "Time Resolved Photoluminescence in InP Doping Superlattices," R. Ranganathan, M. Gal, J.M. Viner and P.C. Taylor, in The Physics of Semiconductors, Vol. 1, O. Engström, ed. (World Scientific, Singapore, 1987), p. 763.
- 83-K-0535-11: "Electron Spin Resonance Studies of Amorphous Semiconductors," P.C. Taylor, C. Lee, J. Hautala and W.D. Ohlsen, in Amorphous Semiconductors, H. Fritzsche, D. Han and C.C. Tsai, eds. (World Scientific, Singapore, 1987), p. 91.
- 83-K-0535-12: "On the Relationship Between ESR and Photodarkening in Glassy As_2S_3 ," J. Hautala, J.Z. Liu and P.C. Taylor, in Disordered Semiconductors,

1 2

- M.A. Kastner, G.A. Thomas and S.R. Ovshinsky, eds. (Plenum, N.Y., 1987), p. 163.
- 83-K-0535-13: "Determination of Critical Thickness in $In_xGa_{1-x}As/GaAs$ Heterostructures by x-ray Diffraction and Photoluminescence Measurements," P.J. Orders, B.F. Usher, M. Gal and P.C. Taylor, SPIE Proc., Bay Point, FL, March 1987, 792, G.H. Döhler and J.N. Schulman, eds. (SPIE, Bellingham, WA, 1987), p. 309.
- 83-K-0535-14: "Chalcogenide Glasses," Mater. Res. Bull. 12, 36 (1987).
- 83-K-0535-15: "Optical Properties of InP Doping Superlattices Grown by Metal Organic Chemical Vapor Deposition," M. Gal, J.M. Viner, P.C. Taylor, J.S. Yuan and G.B. Stringfellow, J. Vac. Sci. Technol. B5, 504 (1987).
- 83-K-0535-16: "Photoluminescence in Strained InGaAs-GaAs Heterostructures," P.C. Taylor, M. Gal, B. Usher and P.J. Orders, J. Appl. Phys. 62, 3898 (1987).
- 83-K-0535-17: "Exciton Binding Energies in GaInAs/InP Quantum Wells Determined by Thermally Modulated Photoluminescence," Z.H. Lin, T.Y. Wang, G.B. Stringfellow and P.C. Taylor, Appl. Phys. Lett. 52, 1590 (1988).
- 83-K-0535-18: "Thermal Modulation of Photoluminescence in $InP/Ga_{0.47}In_{0.53}As/InP$ Quantum Wells," Z.H. Lin, T.Y. Wang, P.C. Taylor and G.B. Stringfellow, J. Vac. Sci. Technol. B6, 1224 (1988).
- 83-K-0535-19: "Optically Induced Electron Spin Resonance in As_xS_{1-x} ," J. Hautala, W.D. Ohlsen and P.C. Taylor, Phys. Rev. B38, 11048 (1988).
- 83-K-0535-20: "Optically Detected Magnetic Resonance Study of Antisite-to-Acceptor and Related Recombination Processes in as-Grown InP:Zn," L.H. Robins, P.C. Taylor and T.A. Kennedy, Phys. Rev. B38 13227 (1988).
- 83-K-0535-21: "Valence and Conduction Band Discontinuities and Exciton Binding Energies in InP/GaInAs/InP Strained Quantum Wells," Z.H. Lin, Y.T. Wang, G.B. Stringfellow and P.C. Taylor, in Proc. 19th Int. Conf. on the Physics of Semicond. (1988).
- 83-K-0535-22: "The Effects of Thermally Modulated Photoluminescence on Optically Detected Magnetic Resonance Experiments," I. Viohl, M.C. DeLong, P.C. Taylor and W.D. Ohlsen, Phys. Rev. B (1989), submitted.
- 83-K-0535-23: "Laser Spectroscopy of Amorphous Semiconductors," P.C. Taylor, in Laser Spectroscopy of Solids, Vol. 2, W.M. Yen, ed. (Springer-Verlag, New York, 1989), p. 257.
- 83-K-0535-24: "Band Offsets and Strained Layer Heterostructures," Z.H. Lin, P.C. Taylor, T.Y. Wang and G.B. Stringfellow, J. Vac. Soc. and Technol. B7, 824 (1989).
- 83-K-0535-25: "Excitation Intensity Dependence of Photoluminescence in Ordered $Ga_{51}In_{49}P$," M.C. DeLong, P.C. Taylor, J.M. Olson and A.E. Kibbler, J. Appl. Phys. (1990), submitted.

TABLE OF CONTENTS

	Page
CUMULATIVE LIST OF PUBLICATIONS	3
I. INTRODUCTION	5
II. PHOTOLUMINESCENCE IN STRAINED InGaAs-GaAs HETEROSTRUCTURES	6
III. EXCITON BINDING ENERGIES IN InP/GaInAs/InP SINGLE QUANTUM WELLS	10
IV. ODMR IN InP	14
V. THERMALLY MODULATED PL AND ODMR	18
VI. SUMMARY	23
REFERENCES	29

1. Date	2. Date
3. S. C.R. #	<input checked="" type="checkbox"/>
4. T. #	<input type="checkbox"/>
5. C. #	<input type="checkbox"/>
6. J. #	<input type="checkbox"/>
7. Date	8. Date
By <i>perl</i>	
Dist. <i>perl</i>	
4. Activity Codes	
5. Activity	6. Activity
Dist. <i>perl</i>	Dist. <i>perl</i>
A-1	



I. INTRODUCTION

The research performed under this contract includes several topics. The first topic is an examination of defects and impurities in III-V binary, ternary and quaternary semiconducting films made by the organometallic vapor phase epitaxial(OMVPE) technique. The second topic is an investigation of III-V multilayers and quantum well structures. A third topic is an investigation of photo-induced structural changes in amorphous semiconductors. All three topics utilized optical and magnetic resonance techniques especially designed for thin-film geometries. The important experimental techniques included electron spin resonance (ESR), nuclear magnetic resonance (NMR), optically-pumped NMR and ESR, optically detected magnetic resonance (ODMR), photoluminescence (PL), optical absorption and various modulated optical spectroscopies such as thermally modulated PL.

The roles of defects and impurities are important to understand in electronically important semiconductors in order to optimize existing electronic devices and to create new devices. Of particular importance for this contract are systems such as GaAs, InP, GaInAs, GaAsSb, and GaInAsP grown by the OMVPE technique.

Layer structures and quantum wells are now readily available in films grown by the OMVPE technique. These structures have potential applications in both high speed devices and in infrared laser applications. As the layer thicknesses get smaller and smaller, the optical and electronic properties of the films change dramatically.

Thin films of such amorphous semiconductors as As_2S_3 undergo structural changes after irradiation with light. These so-called photostructural changes are potentially technologically useful because the etch rates are different in the exposed and unexposed regions. In order to optimize these effects one must first understand the basic mechanisms for the photostructural changes. The approach used to investigate these problems has been to employ experimental probes of the local order, such as magnetic resonance, optical spectroscopy or a combination of these two techniques. The materials studied have been those of technological importance for small scale electronic devices, for lasers, for filters or for other infrared devices. The experimental apparatus has been especially developed and designed for thin-film geometries.

II. PHOTOLUMINESCENCE IN STRAINED InGaAs-GaAs HETEROSTRUCTURES

Using PL techniques we have recently determined the critical layer thicknesses for a range of strained-layer compositions in the system $In_xGa_{1-x}As$ -GaAs. These critical thicknesses have been compared with similar values measured on the same layers by double-crystal x-ray diffraction. Both techniques give essentially the same results.

Recent interest in strained-layer superlattices (SLS) and single quantum wells (SQW) has been motivated by their potential for high-speed and optoelectronic device applications.^{1,2} Strained-layer heterostructures allow the use of lattice mismatched alloys, such as InGaAs-GaAs, without the generation of misfit dislocations. This freedom from the need for precise lattice matching broadens the choice of compatible alloys and increases the ability to tailor the electronic and optical properties of such structures. However, the layer thicknesses d of the mismatched materials have to be thinner than some strain-dependent critical value h_c so that the lattice mismatch is entirely taken up by elastic strain. Although there has been considerable work on the properties of strained-layer structures, the value of the critical thickness is still a matter of controversy.^{3,4} In particular, double-crystal x-ray diffraction measurements of InGaAs/GaAs single heterostructures⁴ give values of h_c that differ by a factor of 4 from those determined by low-temperature photoluminescence (PL) measurements of InGaAs/GaAs single quantum well heterostructures⁵ and SLS's.⁶ It is of interest, therefore, to determine whether PL measurements of h_c give the same results as those from double-crystal x-ray diffraction measurements using the same InGaAs/GaAs single heterostructures for both experiments.

The PL spectra of $In_{0.25}Ga_{0.75}As$ -GaAs single heterostructures are shown in Fig. 1 for representative layer thicknesses. The peak at approximately 820 nm, which is observed for the thinnest samples, arises from the luminescence of the GaAs substrate. Luminescence from the InGaAs layers consists of a single peak which shifts to lower energy as the layer thickness increases. This shift in the position with increasing thickness is also accompanied by an increase in the full width at half maximum (FWHM) of the peak. The broader FWHM in the thicker samples is indicative of the degradation of the structural quality following dislocation formation.

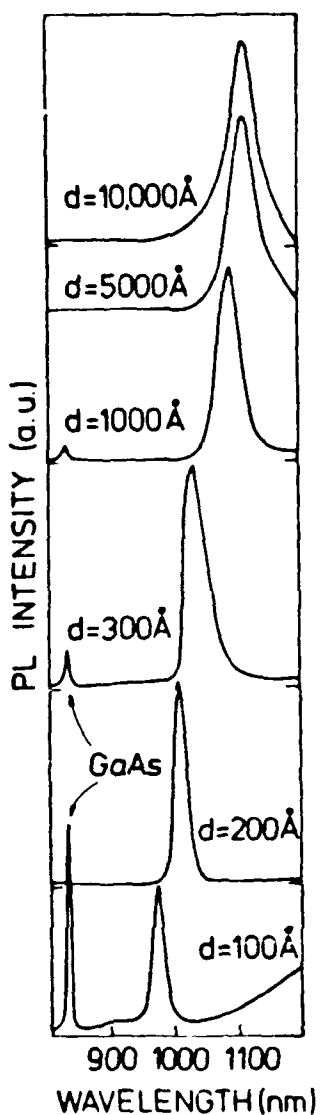


Fig. 1. Low-temperature ($T = 10$ K) photoluminescence spectra of $\text{In}_{0.25}\text{Ga}_{0.75}\text{As}-\text{GaAs}$ single heterostructures of different layer thickness d .

The PL intensity of the InGaAs peak is found to decrease gradually with increasing layer thickness for all compositions studied. For example, the peak intensity in the $d = 200$ Å spectrum with $x = 0.25$ is approximately 400 times more intense than that in the 10,000-Å spectrum. These results are in marked contrast with the dramatic decrease in intensities beyond the critical thickness that is observed in InGaAs/GaAs SLS's⁶ and single quantum wells SQW.⁵ It indicates that the crystalline quality of the epilayer is better preserved beyond h_c in the single heterostructure than in the SLS's and SQW's.

The shift in the PL peak energy is due to biaxial (parallel to [010] and [001]) elastic strain and, in the thinner samples, to quantum size effects. Elastic strain results from the epilayer maintaining registry with the substrate such that the lattice mismatch is accommodated entirely by elastic strain. After correcting for quantum size effects, the PL peak is expected to be at a constant strain shifted position for epilayer thicknesses less than the critical thickness and to move toward the unstrained bulk position beyond the critical thickness as the introduction of misfit dislocations, at first partially, then fully, relieves the strain in the epilayer. The layer thickness at which the strain-shifted PL peak begins to move towards the unstrained bulk position becomes then a measure of the critical layer thickness beyond which misfit dislocations are introduced.

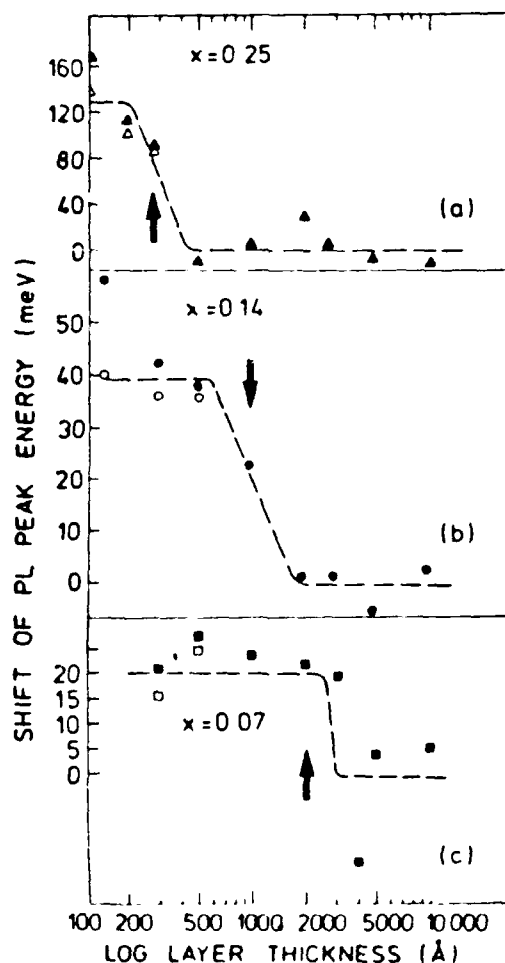


Fig. 2. Shift of PL peak energy as a function of layer thickness. Full symbols represent measured values, while open symbols represent peak energies corrected for quantum size effect. Solid line is aid to the eye. Arrow represents critical layer thickness as determined by double-crystal x-ray diffraction.

The shift in the PL peak position as a function of epilayer thickness is plotted in Fig. 2 for In mole fractions of 0.07, 0.14 and 0.25. The peak shift is measured relative to the unstrained samples. The scatter among the points is mainly due to the spatial variation in the In mole fraction of approximately 0.005 for $x = 0.07$, 0.01 for $x = 0.14$, and 0.015 for $x = 0.25$, which contribute uncertainties of 8, 15 and 20 meV, respectively. The open symbols in the figure represent the PL peak positions after correcting for the quantum size effect, while the full symbols designate the measured values. The first data points to clearly deviate from the strained positions are the 4000-, 1000-, and 500-Å points for the $x = 0.07$, 0.14 and 0.25 cases, respectively. On the basis of the strain-induced PL peak shift it is therefore possible to determine the critical thickness for these structures. It occurs between 2000 and 4000 Å in the $x = 0.07$ case, between 500 and 1000 Å in the $x = 0.14$ case, and between 300 and 500 Å in the $x = 0.25$ case. Scatter in the PL peak position due to experimental uncertainty in the In mole fraction values has meant that critical thicknesses have not been measured with the same accuracy as was possible by structural measurements using double-crystal x-ray diffraction. Nevertheless, within the experimental uncertainty, the PL measurements of h_c yield essentially the same results as the x-ray measurements.⁷

III. EXCITON BINDING ENERGIES IN InP/GaInAs/InP SINGLE QUANTUM WELLS

Studies of the absorption⁸ and photoluminescence (PL)⁹ for quantum well structures in the AlGaAs/GaAs system have been an active area of investigation for several years. It has been found that the quantum well PL is dominated by exciton transitions to much higher temperatures than for bulk materials. This has come to be understood in terms of the compression of the electron and hole wave functions in the quantum well giving a larger overlap and hence a stronger binding energy.^{10,11} For the initial, infinite well calculations, the exciton binding energy increases monotonically as the well width L_z is reduced until reaching a value for the two-dimensional system of four times the bulk value, i.e., approximately 24 meV for the GaAs/AlGaAs quantum wells. Using PL excitation spectroscopy (PLE), such a trend has been observed for wells varying in thickness from 42 to 145 Å.

Recently we have demonstrated that thermally modulated PL (TMPL) may also be used to determine the exciton binding energy.¹² For the GaInAs/InP system, we reported a monotonic increase in exciton binding energy with decreasing well width to nominal well widths of approximately 65 Å. Graded interfaces in the early organometallic vapor phase epitaxial (OMVPE)-grown wells prohibited investigation of the exciton binding energy at smaller well widths. More recently, the OMVPE growth technique has progressed to the point that atomically abrupt interfaces have been achieved. Wells with nominal widths as thin as 10 Å are reported with narrow PL spectra.^{13,14} We have now observed a maximum in exciton binding energy with decreasing well width.

The PL and TMPL spectra for a sample having a nominal well width of 100 Å, determined from the macroscopic growth rate of 3 Å/s, are shown in Fig. 3. The single PL peak is seen to be composed of two TMPL peaks with opposite signs. The TMPL peaks have typical intensities approximately 10^{-2} of the corresponding PL peak intensities. The derivative TMPL spectrum allows a separation into transitions with opposite dependences of intensity on temperature. An increase in temperature results in a decrease in exciton concentration, hence an increase in the free-carrier concentration. Thus, an increase in

temperature results in a decrease in exciton recombination, and an increase in free-carrier recombination. The relatively broad PL peak in Fig. 2 can be resolved into two component TMPL peaks. The higher energy, positive peak is due to free electron and hole recombination and the negative peak is due to exciton recombination. The separation of 6 meV yields an estimate of the exciton binding energy at this well width (100 Å). However, as discussed by Gal et al.,¹² a more accurate value of exciton binding energy can be obtained by fitting the results of a simple model calculation to the TMPL spectrum with the exciton binding energy as an adjustable parameter. This analysis shows that the TMPL peak separation is always greater than or equal to the actual exciton binding energy. For many of our spectra involving the participation of regions with several quantum well widths, a simple calculation cannot be used to fit the experimental data. Thus, we use the peak separation as an upper limit of the exciton binding energy. This difficulty will not affect the qualitative features of exciton binding energy versus well widths. Also shown in Fig. 3 are the PL and TMPL spectra for a quantum well with a nominal width of 18 Å. The extra structure in this spectrum is discussed elsewhere.¹⁵

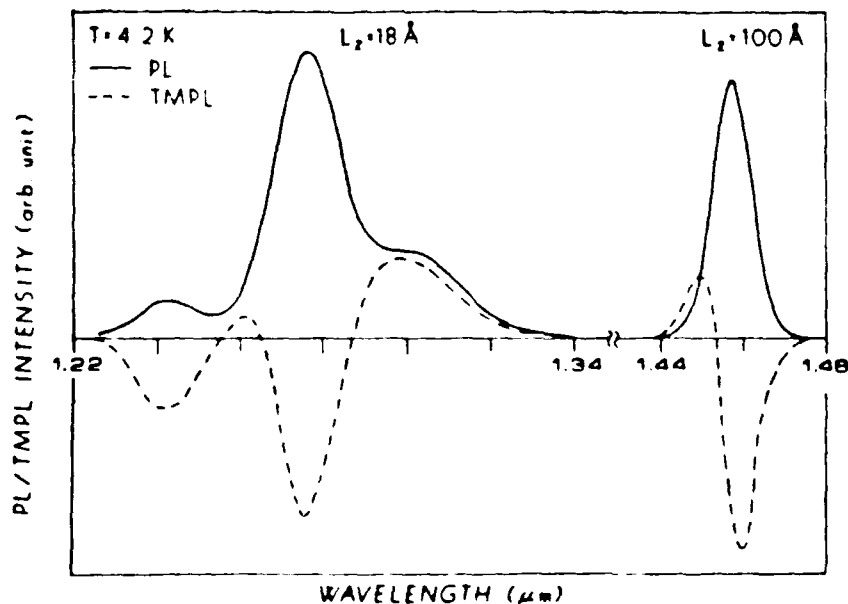


Fig. 3. Photooluminescence and thermally modulated photoluminescence spectra for two InP/GaInAs/InP quantum wells with nominal thicknesses of 100 and 18 Å. The measurements were performed at approximately 2 K.

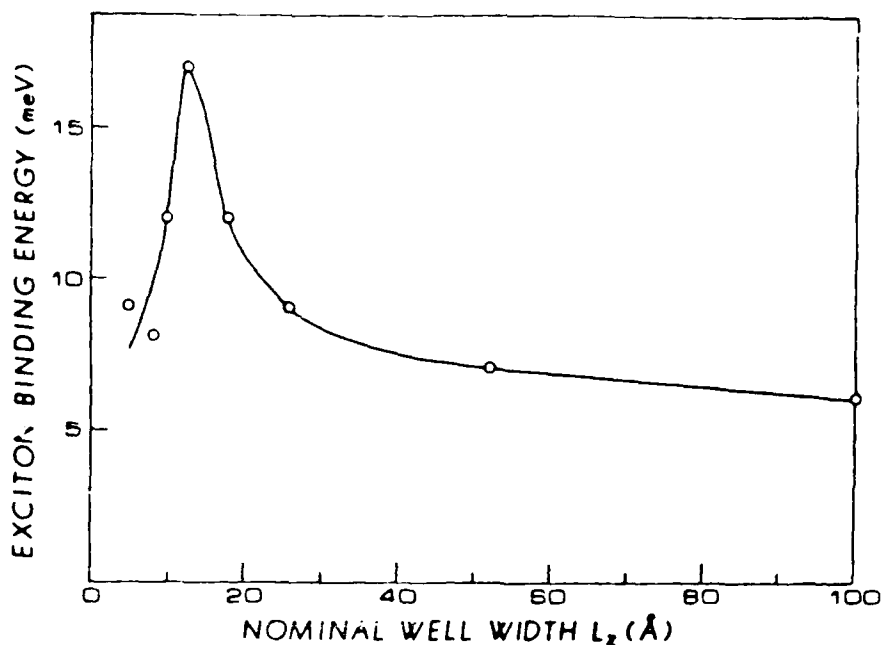


Fig. 4. Dependence of exciton binding energy, measured as the difference in peak energies for free and exciton recombination in the thermally modulated photoluminescence spectra, on nominal well width for InP/GaInAs/InP quantum wells.

Similar results have been obtained for other samples with nominal well widths in the range from 3 to 100 Å. The PL consists of a doublet, or triplet, due to the presence of two, or three, well widths, differing in thickness by a single monolayer, sampled simultaneously by the excitation beam.¹⁵ In all cases the PL is much stronger than for thick GaInAs layers and the PL half widths are narrow. For each well, the separation between the TMPL peaks for free electron-hole and exciton recombination allows an estimation of the exciton binding energy. The values determined in this way are plotted versus nominal well width in Fig. 4. For the thickest well, having a nominal width of 100 Å, the exciton binding energy of approximately 6 meV corresponds closely with the value observed from absorption measurements on 110 Å AlInAs/GaInAs wells reported by Weiner et al.¹⁶ and the TMPL results of Gal et al.¹² who reported a value of 7 meV for a 100 Å GaInAs/InP quantum well. This gives confidence that the simple expedient of using the TMPL peak separation as a measure of the exciton binding energy does not produce large errors.

As expected and observed earlier,¹² the exciton binding energy increases with decreasing well width. However, we observe a peak occurring at a nominal well width of approximately 13 Å with a maximum exciton binding energy of approximately 17 meV. A sharp decrease in exciton binding energy is observed for thinner quantum wells.

IV. ODMR IN InP

The P_{In} antisite in InP was first identified by conventional electron paramagnetic resonance¹⁷ (EPR or ESR) in an electron-irradiated, liquid-encapsulated, Czochralski-grown single crystal, and subsequently by two different optically detected magnetic resonance¹⁸⁻²⁰ (ODMR) techniques. ODMR has been one of the most useful probes of the atomic and electronic structure of antisites and other intrinsic defects in semiconductors, for the following reasons. While conventional EPR is restricted to stable or metastable paramagnetic states, optically detected magnetic resonance (ODMR) can be applied to defects with short-lived paramagnetic excited states and nonmagnetic ground states. In addition, while conventional EPR generally requires more than 10^{15} spins/cm³ in order to observe a resonance, even in bulk samples, ODMR is potentially sensitive to a much smaller concentration of defects.

More recently, the resonance of the antisite in nonirradiated zinc-doped LEC-grown InP was observed²¹ by PL ODMR, and, in addition, a new antisite-defect complex was identified by the same technique in phosphorus-annealed InP.²² In all of the above PL ODMR studies, the antisite resonance was observed as enhancing a deep PL band at 0.8-0.9 eV. (The antisite-related PL appears to dominate the total deep-level PL emission spectrum in heavily electron-irradiated InP, but is only seen as a small shoulder on top of the other deep-level PL bands in the as-grown samples.^{20,21})

We have shown²³ that the antisite resonance in as-grown InP:Zn can be observed both as an enhancing resonance of the deep-level PL at 0.8 eV and as a quenching resonance, of approximately equal magnitude, of the shallow-donor to acceptor PL at 1.37 eV. Other ODMR signals have also been detected at 1.37 eV.

ODMR spectra obtained by monitoring the P_{In} -antisite-related PL at 0.8 eV and the shallow-donor to acceptor PL at 1.37 eV are shown in Figs. 5(a) and 5(b), respectively. For conciseness, the antisite resonance detected at 0.8 eV will be denoted the antisite-antisite (AS-AS) resonance, and the antisite resonance detected at 1.37 eV will be denoted the antisite-donor-acceptor (AS-DA) resonance. The AS-DA resonance is observed with better

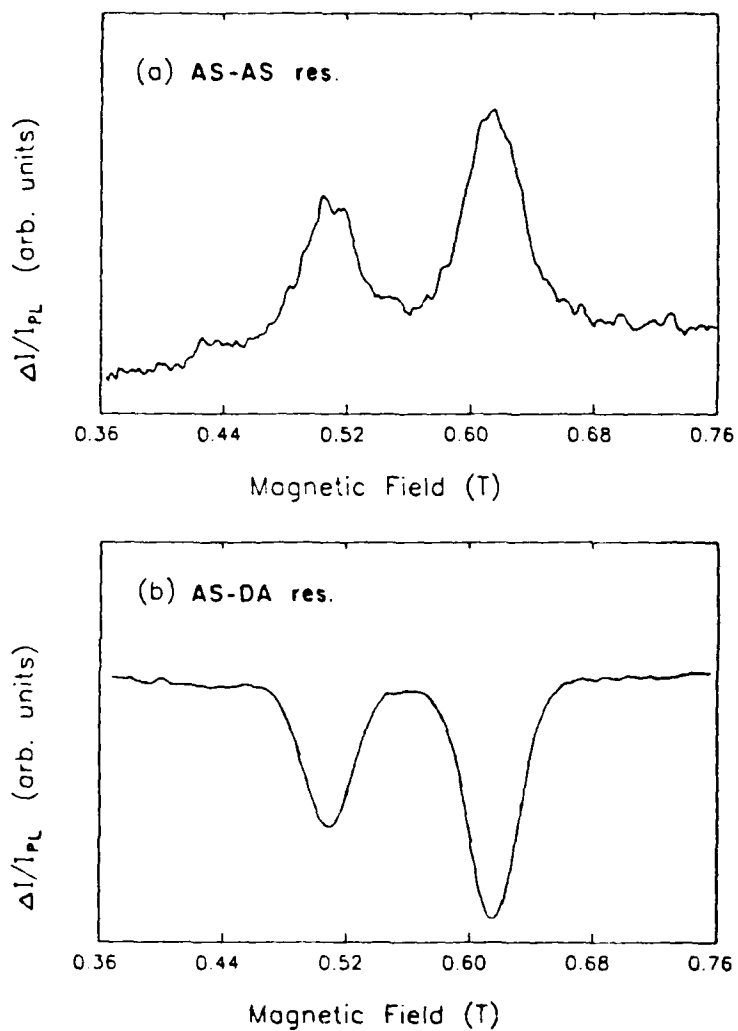
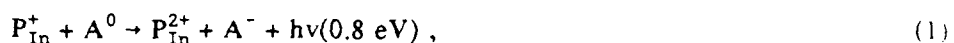


Fig. 5. (a) Spectrum of the antisite ODMR enhancing the antisite to acceptor PL at 0.8 eV. Spectrum shown here was obtained by averaging many individual spectra, with photoexcitation intensity, 1 W/cm²; microwave resonance frequency, 15.9 GHz; microwave power, 20 mW; variable modulation frequency. (b) Spectrum of the antisite ODMR quenching the shallow-donor to acceptor PL at 1.37 eV, obtained by averaging many individual spectra; other experimental parameters same as for (a).

signal-to-noise than the AS-AS resonance because of the differences in PL intensity and detector sensitivity, but the peak positions and linewidths of the two are equal within experimental uncertainty.

The P_{In} antisite resonance is split into two lines because of the strong hyperfine interaction between the electron spin and the central $^{31}P(I = \frac{1}{2})$ nucleus. Unresolved ligand hyperfine interactions give rise to the large linewidth (0.039 T) of each component.

The observation that the antisite resonance quenches the shallow donor to acceptor PL at 1.37 eV provides support for the model of Deiri et al.,¹⁸ according to which the antisite-related PL at 0.8 eV, at least in p-type material, arises from the recombination of an electron bound to an antisite with a hole bound to an acceptor. Antisites and shallow donors may then be competing recombination centers for acceptor-bound holes. The recombination processes may be written as



Here, P_{In}^+ is the paramagnetic state of the antisite, occupied by one electron, and P_{In}^{2+} is the nonmagnetic fully ionized state. Similarly, D^0 is the neutral state of the donor, occupied by one electron, A^0 is the neutral state of the acceptor, occupied by one hole, and D^+ and A^- are the

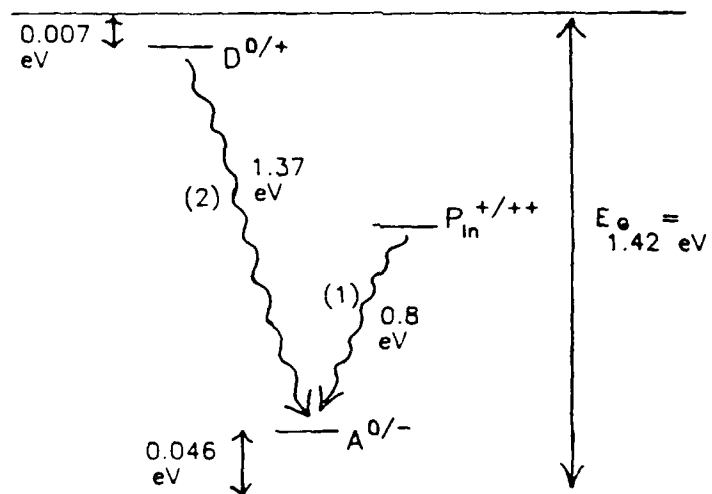


Fig. 6. Energy-level diagram showing the antisite ($P_{In}^{+/2+}$), shallow-donor ($D^{0/+}$), and zinc-acceptor [$A^{0/-}$ (Zn)] states in the band gap of InP and the two competing recombination processes: the antisite to acceptor transition (1) and the shallow-donor to acceptor transition (2).

ionized states of the donor and acceptor. An energy-level diagram illustrating the competing recombination processes (1) and (2) is presented in Fig. 6.

It is assumed that the antisites and shallow donors are fully compensated by Zn acceptors; thus all of the donor levels are fully ionized in the ground state (D^+ and P_{In}^{2+}). This assumption is consistent with the observation that too few antisites are paramagnetic (P_{In}^0) in the ground state to observe by EPR or MCD ODMR. It is also assumed that the doubly occupied state of the antisite (P_{In}^+), if present at all, does not have a significant effect on the recombination processes studied by ODMR. At high photoexcitation intensities, conduction-band to acceptor recombination may become an important process. The band to acceptor PL occurs at slightly higher photon energy than the shallow-donor to acceptor PL (1.378 eV versus 1.373 eV); the two transitions generally give rise to one unresolved peak in the PL spectrum.

V. THERMALLY-MODULATED PL AND ODMR

Optically detected magnetic resonance (ODMR) is a well established method of investigation of spin-dependent recombination processes in crystalline and amorphous solids. In ODMR, electron spin resonance in an excited state of a defect center is detected as a relative change in the intensity or polarization of the recombination radiation. Since ODMR combines the relatively weak magnetic resonance phenomenon with the strongly spin-dependent optical transitions to measure the change in emission intensity or polarization it is potentially a very sensitive technique. In an ideal experiment the sample would be subjected only to the microwave magnetic field of the resonant cavity. Due to its finite size, however, the sample is also exposed to the microwave electric field. In a microwave modulated ODMR experiment this "spurious" electric field can result in a modulation of the sample temperature and thus to a simultaneous temperature modulation of the photoluminescence intensity. Since the microwave and temperature modulation frequencies are the same, a phase sensitive technique will detect changes in the photoluminescence intensity due to both, magnetic resonance (intended), as well as temperature modulation (unintended). Temperature modulated photoluminescence (TMPL) spectroscopy in itself has been developed into a technique for investigating recombination processes in semiconductors.¹⁵ In the earlier stages of this development, the sample was mounted on a thin film resistor to modulate the sample temperature.^{24,25} Now the sample is placed in a specially designed microwave cavity, in which the maximum of the microwave electric field coincides with the sample position and the sample temperature is modulated via microwave heating.^{26,27}

In some materials zero magnetic field and non-resonant background signals have been observed in ODMR^{23,28,29} (e.g., the experiments described in the previous section) and optically detected cyclotron resonance (ODCR)³⁰ experiments. The magnitudes of both effects generally vary with the experimental conditions, in particular microwave power and photo-excitation intensity. The zero field signal can be orders of magnitude larger than the actual ODMR signal and effectively mask it. A typical example is the ODMR spectrum of InP:Zn, shown in Fig. 7(a), where at low photoexcitation (bottom curve in Fig. 7(a)) the

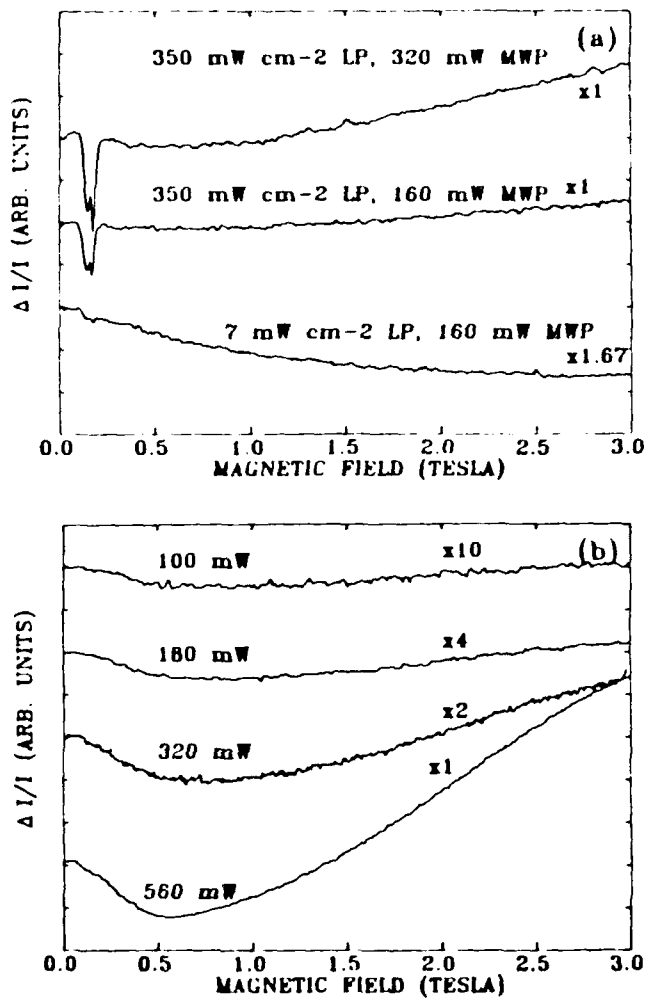


Fig. 7. (a) All light 3 GHz "ODMR" of InP:Zn at different microwave powers (MWP) and photoexcitation intensities (LP). The zero field signals are $\Delta I/I = -0.46\%$, -0.12% and -0.65% for the top to bottom curves, respectively and the vertical scale is $\sim 0.018\%$ per tic mark for all curves. The large zero field offsets were omitted for the purpose of presentation. The zero levels are therefore arbitrary, however, all curves are plotted on the same scale. (b) All light 3 GHz "ODMR" of InP at different microwave powers. The zero field signals are $\Delta I/I = -0.05\%$, -0.14% , -0.37% and -0.35% for the top to bottom curves, respectively and the vertical scale is $\sim 0.43\%$ per tic mark. The zero field signal is included, however, the zero of each curve was chosen arbitrarily.

fractional change in the PL-intensity is $\Delta I/I = -0.655\%$ at magnetic resonance (~ 0.2 Tesla) and -0.65% at zero magnetic field. Since the ODMR signal is much weaker than the zero field signal it is necessary to compensate for the latter. But the large magnitude of the zero field signal may require a reduction in sensitivity, thereby making an ODMR measurement much more difficult. At higher photo-excitation intensities (top curves of Fig. 7(a)) the

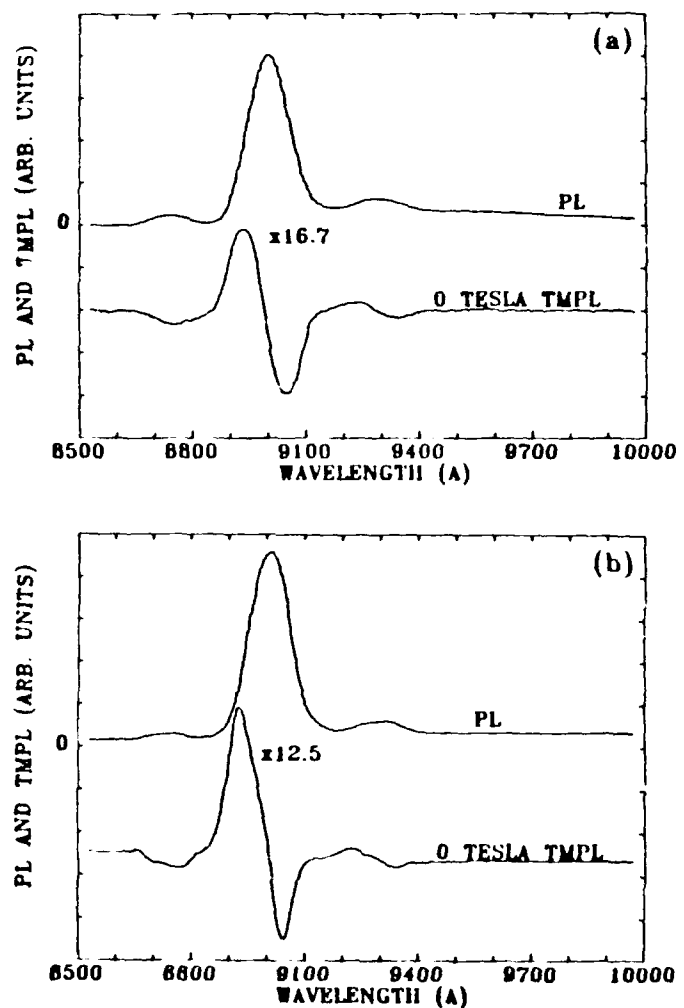


Fig. 8. Incorrect PL and TMPL spectra of the undoped InP in the (a) 3 GHz and (b) 16 GHz configuration. Magnetic field dependence of the undoped InP TMPL spectrum (c) at 560 mW microwave power in the 3GHz configuration and (d) at 30 mW power in the 16 GHz configuration. For the purpose of presentation the curves were displaced an integral multiple of 2 units.

ODMR signal is easily observed because it is only a factor of 10 weaker than the zero field signal. A second example is shown in Fig. 7(b) for undoped InP. No magnetic resonances are observed, yet large non-resonant signals up to $\Delta I/I \approx -0.35\%$ at zero magnetic field and $+1.5\%$ at 3 Tesla (bottom curve of Fig. 7(b)) are present, demonstrating a strong magnetic field dependence of these signals under certain experimental conditions. Also note the gross similarity between the non-resonant signals in the two samples in Fig. 7 (InP:Zn and undoped InP). We have correlated these zero field and non-resonant signals to a temperature

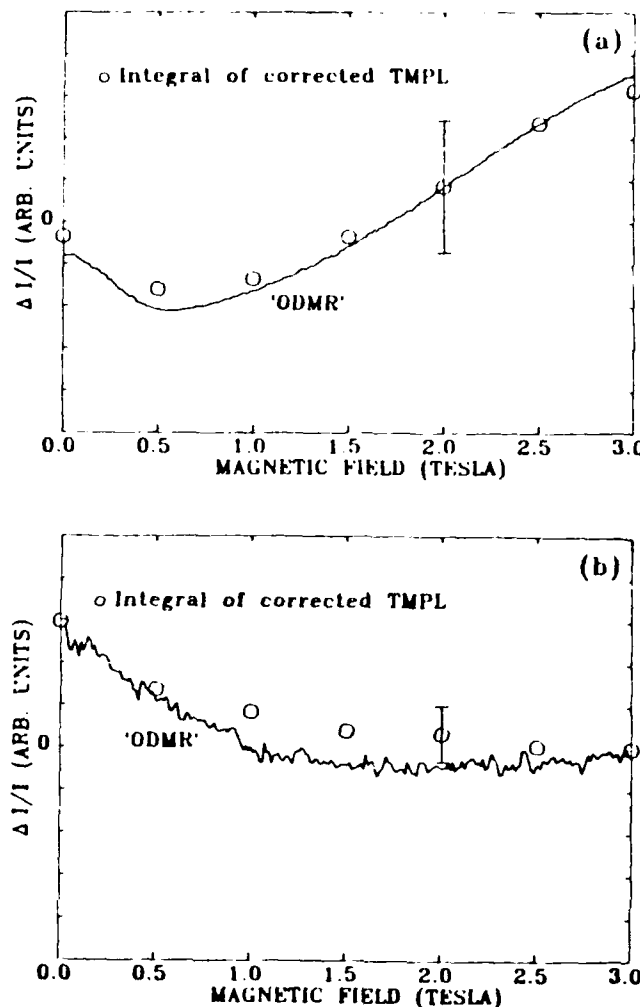


Fig. 9. Comparison between the "all light ODMR" spectrum (solid curve) and the magnetic field dependent integral of the corrected InP TMPL spectra (open circles) at 3 GHz and 16 GHz, respectively. The zeros shown are absolute and the curves include the zero field signals. The error bar indicates for a representative point the error in the numerical integration of the TMPL and PL spectra due to uncertainties in the choice of the baseline.

modulation of the photoluminescence which is induced by the microwave electric field of the resonant cavity.

The TMPL spectra of InP, shown in Fig. 8(a) and 8(b), were obtained using the 3 GHz and 16 GHz ODMR cavities, respectively. These spectra are in excellent agreement with those acquired in TMPL experiments using the resistive heating technique. The spectral resolution ($\sim 100 \text{ \AA}$) of these experiments is not good enough to define the TMPL line shapes accurately for all features, but this resolution was chosen because it corresponds to that which is commonly employed for the ODMR measurement on these samples. It should be pointed

VI. SUMMARY

Recent interest in strained-layer superlattices and quantum wells has been motivated by their potential for high-speed devices. Although there has been considerable work on strained layer heterostructures, the values of the critical thicknesses are still a matter of controversy. Our PL measurements have demonstrated a useful diagnostic technique to measure critical thicknesses in strained layer heterostructures.

In single quantum wells the binding energies of excitons are expected to increase as the well widths decrease because of quantum confinement of the excitons. As the wells decrease further, the binding energies are expected to decrease once again as the lowest energy level in the quantum well approaches the barrier energy and the wave function spills out into the barrier layer. Our thermally modulated photoluminescence measurements on InP/GaInAs/InP single quantum wells where the well widths are as small as about 3 μ m have demonstrated this trend for the first time.

The P_{In} antisite in InP was first identified by ESR. Our recent ODMR experiments have discovered a quenching resonance for the P_{In} antisite by monitoring the shallow donor-acceptor (Zn) PL in Zn-doped InP. Because this ODMR can be observed with much better signal to noise than the primary enhancing resonance, the commonly accepted model can be tested in more detail. This model¹⁸ is confirmed by the present results.

There is often an annoying non-resonant background signal in ODMR studies of III-V semiconductors. We have shown that this non-resonant background is due to a thermal modulation of the PL. Detailed analyses of this thermally-modulated PL signal have demonstrated that the background signals so often observed in ODMR in semiconductors are in fact thermal in origin. These thermal signals result from a temperature modulation of the photoluminescence induced by the microwave electric fields of the ODMR cavity.

Revised 10/27/86
Experiments on InP/GaInAs/InP
using ESR and PL

7

REFERENCES

1. M.D. Camras, J.M. Brown, N. Holonyak, Jr., M.A. Nixon, R.W. Kaliski, M.J. Ludowise, W.T. Dietze, and C.R. Lewis, *J. Appl. Phys.* **58**, 6183 (1983).
2. J.J. Rosenberg, M. Benlamri, P.D. Kircher, J.N. Woodall, and G.D. Pettit, *IEEE Electron Device Lett.* **EDL-6**, 491 (1985).
3. B.W. Dodson and P.A. Taylor, *Appl. Phys. Lett.* **49**, 642 (1986).
4. P.J. Orders and B.F. Usher, *Appl. Phys. Lett.* **50**, 980 (1987).
5. N.G. Anderson, W.D. Laidig, R.M. Kolbas, and V.C. Lo, *J. Appl. Phys.* **60**, 2361 (1986).
6. A.F.S. Penna, J. Shah, T.Y. Chang, and M.S. Burroughs, *Solid State Commun.* **51**, 425 (1984).
7. M. Gal, P.C. Taylor, B.F. Usher and P.J. Orders, *J. Appl. Phys.* **62**, 3898 (1987).
8. R. Dingle, *Festkoerper-probleme (Advances in Solid State Physics)*, edited by H.J. Queisser (Pergamon Vieweg, Bruanschweig, 1975), Vol. XV, p. 21.
9. B.A. Vojak, N. Holonyak, Jr., D.W. Laidig, K. Hess, J.J. Coleman, and P.D. Dapkus, *Solid State Commun.* **35**, 477 (1980).
10. R.C. Miller, D.A. Kleinman, W.T. Tsang, and A.C. Gossard, *Phys. Rev. B* **24**, 1134 (1981).
11. R.L. Greene and K.K. Bajaj, *Solid State Commun.* **45**, 831 (1983).
12. M. Gal, C.P. Kuo, B. Lee, R. Ranganathan, P.C. Taylor, and G.B. Stringfellow, *Phys. Rev. B* **34**, 1356 (1986).
13. T.Y. Wang, K.L. Fry, A. Persson, E.H. Reihlen, and G.B. Stringfellow, *Appl. Phys. Lett.* **52**, 290 (1988).
14. T.Y. Wang, K.L. Fry, A. Persson, E.H. Reihlen, and G.B. Stringfellow, *J. Appl. Phys.* **63**, 2674 (1988).
15. Z.H. Lin, T.Y. Wang, G.B. Stringfellow, and P.C. Taylor, *Appl. Phys. Lett.* **52**, 1590 (1988).
16. J.S. Weiner, D.S. Chemla, D.A.B. Miller, T.H. Wood, D. Sivco, and A.Y. Cho, *Appl. Phys. Lett.* **46**, 619 (1985).
17. T.A. Kennedy and N.D. Wilsey, *Appl. Phys. Lett.* **44**, 1089 (1984).
18. M. Deiri, A. Kana-ah, B.C. Cavenett, T.A. Kennedy, and N.D. Wilsey, *J. Phys. C* **17**, L793 (1984).
19. A. Kana-ah, M. Deiri, B.C. Cavenett, N.D. Wilsey, and T.A. Kennedy, *J. Phys. C* **18**, L619 (1985).
20. B.C. Cavenett, A. Kana-ah, M. Deiri, T.A. Kennedy, and N.D. Wilsey, *J. Phys. C* **18**, L473 (1985).
21. T.A. Kennedy and N.D. Wilsey, *J. Cryst. Growth* **83**, 198 (1987).

22. T.A. Kennedy, N.D. Wilsey, P.B. Klein, and R.L. Henry, *Mater. Sci. Forum* **10-12**, 271 (1986).
23. L.H. Robins, P.C. Taylor and T.A. Kennedy, *Phys. Rev.* **38**, 13227 (1988).
24. M. Gal, C.P. Kuo, B. Lee, R. Ranganathan, P.C. Taylor, and G.B. Stringfellow, *Phys. Rev. B* **34**, 1356 (1986).
25. M. Gal, *Phys. Rev. B* **18**, 803 (1978).
26. Z.H. Lin, T.Y. Wang, P.C. Taylor, and G.B. Stringfellow, *J. Vac. Sci. Technol. B* **6**, Jul./Aug. (1988).
27. Z.H. Lin, T.Y. Wang, G.B. Stringfellow, and P.C. Taylor, *Appl Phys. Lett.* **52**, 1590 (1988).
28. B.C. Cavenett, *Adv. in Phys.* **30**, 475 (1981).
29. D.J. Dunstan and J.J. Davies, *J. Phys. C* **12**, 2927 (1979).
30. B.C. Cavenett and E.J. Pakulis, *Phys. Rev. B* **32**, 8449 (1985).